Evaluating the Interactions Between Vibrational Modes and Electronic Transitions Using Frontier Orbital Derivatives

Lisa A. Schröder,[a,b] Harry L. Anderson,[a] Igor Rončević[a]*

Vibrations can significantly affect molecular properties, even at zero Kelvin. Accounting for these effects when using computational modelling is costly, as it requires many calculations at geometries distorted from equilibrium. Here, we propose a low-cost method for identifying vibrations most strongly coupled to the electronic structure, based on using orbital derivatives as a diagnostic.

Predicting the barriers to electronic excitation and charge transfer is essential for engineering materials for solar cells,[1] mimicking redox processes in enzymes,[2] and building molecular electronic devices.[3] Advances in electronic structure theory have enabled accurate descriptions of electronic states and the couplings between them,[4-7] facilitating *in silico* design and screening of potential next-generation molecular devices. However, most work on predicting molecular properties such as vertical excitation energies, polarizabilities, or single-molecule conductances is limited to equilibrium geometries, ignoring effects of nuclear motion.[4, 5, 8, 9] This approach works well when the coupling between electronic states and nuclear motion is small and symmetric. In other words, if movement in direction $+Q$ and $-Q$ (which can be represented as a linear combination of normal modes Q_i) changes some property by a small amount $+\delta$ and $-\delta$, respectively, the effect of nuclear motion can be approximated by a mere broadening (proportional to $d\delta/dQ$) of the observed property.

Recently, Bai et al.[10] demonstrated that this naïve approximation does not always hold by showing that computed vertical excitation energies usually shift to lower energies when effects of nuclear motion are included. Alvertis and collaborators[11] found that this gap renormalization is present even at zero Kelvin (zero-point renormalization, or ZPR), and

estimated its average value to −0.35 eV for Thiel's set[4] of small organic molecules, with extreme cases reaching −1.36 eV. They also noted that ZPR can often be reduced to the effect of only several vibrations. A similar conclusion was reached by Lambropoulos et al., who found that ZPR in cyclo[18]carbon can be reduced to the effect of a few bond-stretching vibrational modes.[12] In organic molecular wires, bond stretching and backbone torsion play a large role, as the electron and hole mobilities are highly dependent on the extend of conjugation modulated by these vibrations.[13-15] In more general cases, it can be challenging to understand which vibrations are important and which can be neglected.

Here, we provide a straightforward, inexpensive method for investigating the effect of individual normal modes on the electronic structure, based on calculating derivatives of frontier orbital energies with respect to molecular vibrations. We first use this method to evaluate how vertical excitation energies are modulated by specific vibrations, and then we analyse the effect of specific vibrations in a system with strong electron-vibration coupling.

In the framework of time-dependent density functional theory (TD-DFT), the first optical transition can usually be attributed to an excitation of a single electron from the highest occupied molecular orbital (HOMO) to the lowest unoccupied molecular orbital (LUMO). The energy difference between the HOMO (E_H) and the LUMO (E_L) can be taken as a measure of the fundamental gap (E_{gap}), which is more rigorously defined as the difference between the ionization potential and the electron affinity.[16] At the equilibrium geometry $Q_{eq} = 0$, the first vertical excitation energy (E_{S1}; also called the optical gap) will differ from the fundamental gap (E_g) by the exciton binding energy (E_{bind}), which is a measure of the Coulombic attraction between the newly formed electron-hole pair:

$$E_{S1}(Q_{eq} = 0) = E_g(0) - E_{bind}(0)$$
$$= E_L(0) - E_H(0) - E_{bind}(0) \quad (1)$$

When the geometry is displaced along a normal mode i by some amount by Q_i, the optical gap changes by:

a. *Department of Chemistry, Oxford University, Chemistry Research Laboratory, Oxford OX1 3TA, United Kingdom. Email: igor.roncevic@chem.ox.ac.uk*
b. *Institute of Physical Chemistry, Karlsruhe Institute of Technology, KIT Campus South, Fritz-Haber-Weg 2, D-76131 Karlsruhe, Germany.*

$$\Delta E_{\mathrm{S1}}(Q_i) = [E_{\mathrm{L}}(Q_i) - \Delta E_{\mathrm{L}}(0)] - [E_{\mathrm{H}}(Q_i) - \Delta E_{\mathrm{H}}(0)] - [E_{\mathrm{bind}}(Q_i) - \Delta E_{\mathrm{bind}}(0)] \quad (2)$$

which can also be written as:

$$\Delta E_{\mathrm{S1}}(Q_i) = \Delta E_{\mathrm{gap}}(Q_i) - \Delta E_{\mathrm{bind}}(Q_i) \quad (3)$$

In practice, the effect of nuclear motion on the S_1 energy ΔE_{S1} is determined by performing a series of excited-state calculations on geometries displaced by Q, which can either be obtained by Monte Carlo sampling (50–100 samples, in which Q for each geometry is a random linear combination of Q_i) or by finite differences (which usually involves displacements by $+Q_i$ and $-Q_i$ for each normal mode i). However, if the exciton binding energy is much less sensitive to geometric changes than frontier orbital energies (i.e. $\Delta E_{\mathrm{b}} << \Delta E_{\mathrm{gap}}$), then the changes in the optical gap due to nuclear motion ΔE_{S1} can be approximated by the change in the fundamental gap ΔE_{gap}. We call this ($\Delta E_{\mathrm{S1}} \approx \Delta E_{\mathrm{gap}}$) the static binding approximation. It is attractive for two reasons. One, it simplifies the evaluation of effects of nuclear movement. When the harmonic approximation is valid (small Q), ΔE_{gap} can simply be calculated from derivatives of orbital energies with respect to normal modes, dE_{H}/dQ_i and dE_{L}/dQ_i, which can be obtained in a single ground-state calculation;[17] in contrast, ΔE_{bind} can only be obtained by many excited-state calculations. Two, the magnitude of orbital energy derivatives enables us to identify the vibrations most strongly coupled to the electronic structure.

To investigate how well the static binding approximation holds, we tested it on the Thiel's set of small organic molecules (Figure 1), for which the ZPR was investigated in ref 11. We computed ΔE_{gap} using orbital derivatives and compared it to ΔE_{S1} obtained using TD-DFT (B3LYP[18]/def2-SVP), calculated for geometries modulated along each normal mode Q_i by the standard deviation of the thermal distribution $\sigma_i(T)$:[11]

$$\sigma_i(T)^2 = \frac{1}{2\omega_i} p_i(T) \quad (4)$$

where ω_i is the vibrational frequency, T is the temperature, and $p_i(T)$ is the Bose-Einstein population at T, which is equal to unity at $T = 0$. Equation (4) gives us a way to account for zero-point vibrations by looking at only two characteristic geometries modulated from the equilibrium by $\pm\sigma_i(0)$, as shown by Hele et al.[11]

We find that the static binding approximation holds reasonably well across Thiel's set (Figures 1 and S1): in 18 out of 30 molecules (Figure 1a–o and S1a–d; green background), all normal modes with a notable ΔE_{S1} can be diagnosed from ΔE_{gap}, with most of these points being close to the $\Delta E_{\mathrm{gap}} = \Delta E_{\mathrm{S1}}$ diagonal (usually $R^2 > 0.8$). In 6 further cases (Figure 1p–u), most vibrations with a significant ΔE_{S1} can be easily identified from ΔE_{gap}, but the importance of a single stretching (~ 1600 cm^{-1}; black arrow in Figure 1p–u) vibration is consistently underestimated. Finally, the static binding approximation does not hold (Figure 1v–x and S1e–f; orange background) in very small molecules due to their tightly bound excitons (e.g. ethene or cyclopropane), and it fails in *7H*-purin-6-amine (Figure 1v), where stretching vibrations modulate the exciton binding in a non-trivial way.
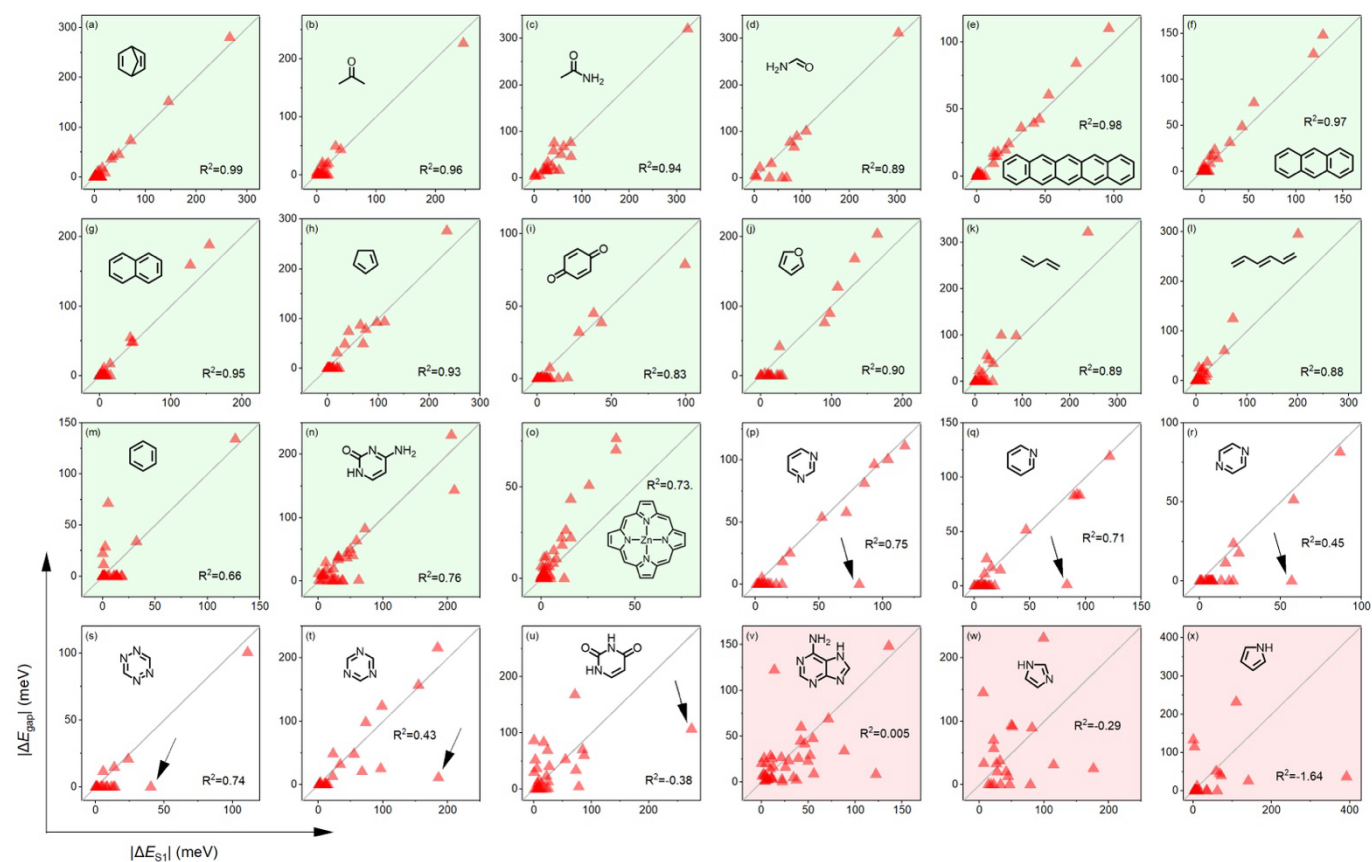

Figure 1. Electronic-vibrational coupling calculated using ΔE_{gap} (vertical axis) and ΔE_{S1} (horizontal axis; both in meV) for selected molecules from Thiel's set, decomposed by normal modes (triangles) and evaluated for zero-point vibrations. Black arrows in (p)-(u) correspond to stretching vibrations with a large ΔE_{S1} relative to ΔE_{gap}. Results for remaining molecules are given in Figure S1.

Our results (Figure 1) illustrate that in most small organic molecules only a few (usually <15%) normal modes are strongly coupled to frontier orbitals. ΔE_{gap} can be used to identify the vibration most strongly coupled to frontier orbitals with high confidence (excluding very small systems), and in the majority of cases it correctly identifies vibrations strongly coupled with electronic structure, without resorting to excited-state calculations. Furthermore, as the exciton binding energy decreases with molecular size,[19] we expect the static binding approximation to be even more accurate in molecules larger than those investigated here. Therefore, when a description of molecular properties beyond the equilibrium geometry is desired, we suggest using ΔE_{gap} to identify normal modes which are likely to affect the electronic structure. A limitation of ΔE_{gap} is that it is harmonic, i.e. it can only determine the size of the orbital coupling, and the calculation of its asymmetry requires excited state calculations.

Accounting for effects of nuclear motion is particularly important in cases of strong electron-vibration coupling. Usually, in organic molecules the electronic transitions (typically $v_{el} > 10,000$ cm^{-1}) are well-separated from vibrational transitions ($v_n \leq 3200$ cm^{-1}), with much broader and more intense signals. In radical cations of π-conjugated porphyrin oligomers this distinction is less clear, with both electronic and vibrational transitions producing very intense signals in the 1500–6000 cm^{-1} region.[20-22] These unusually strong vibrational transitions can be detected using infrared (IR) spectroscopy, and they are usually called IR active vibrations (IRAVs). Recently, IRAVs were experimentally found at ~1330, ~1550 and ~2080 cm^{-1} (shaded area in Figure 1d–f) in the butadiyne-linked porphyrin dimer $\mathbf{1}^{\bullet+}$ (Figure 2a), and tentatively assigned to normal modes shown in Figure 2b. Movement along these IRAVs was attributed to the strong coupling of vibrational modes with the singly occupied molecular orbital (SOMO) orbital.[20] Here, we investigate this coupling in more detail by analysing how normal modes in $\mathbf{1}^{\bullet+}$ modulate orbital energies (Figure 2c–f). Using the same density functional as in previous work (LC-ωPBE[20, 23]), we calculated the couplings between the HOMO and SOMO energies and normal modes in $\mathbf{1}$ and $\mathbf{1}^{\bullet+}$ and compared them with computed dipole moment changes with respect to normal modes (i.e. infrared intensities) dD/dQ_i (Figure 2c–d). Our results show that these frontier orbital derivatives are indeed larger in $\mathbf{1}^{\bullet+}$ than in neutral $\mathbf{1}$ (Figure 2c,d), in agreement with previous work. However, we also note that the contribution of orbitals up to SOMO−3 (Figure 2e) is significant in IRAVs at 1390 cm^{-1} and 2100 cm^{-1}, outweighing the contribution of the SOMO.

While the dipole moment D only depends on the occupied orbitals (within the DFT framework), a proper account of electron-vibration coupling should include the unoccupied orbitals as well. In $\mathbf{1}^{\bullet+}$, we find that the singly unoccupied molecular orbital (SUMO) is also strongly coupled to movement along several vibrations, resulting in a very large ΔE_{gap} (Figure 2d) at the IRAV positions. Therefore, a large ΔE_{gap} may be used as a diagnostic to identify IRAVs and vibrational modes strongly coupled to electronic states, despite being calculated at the equilibrium geometry.
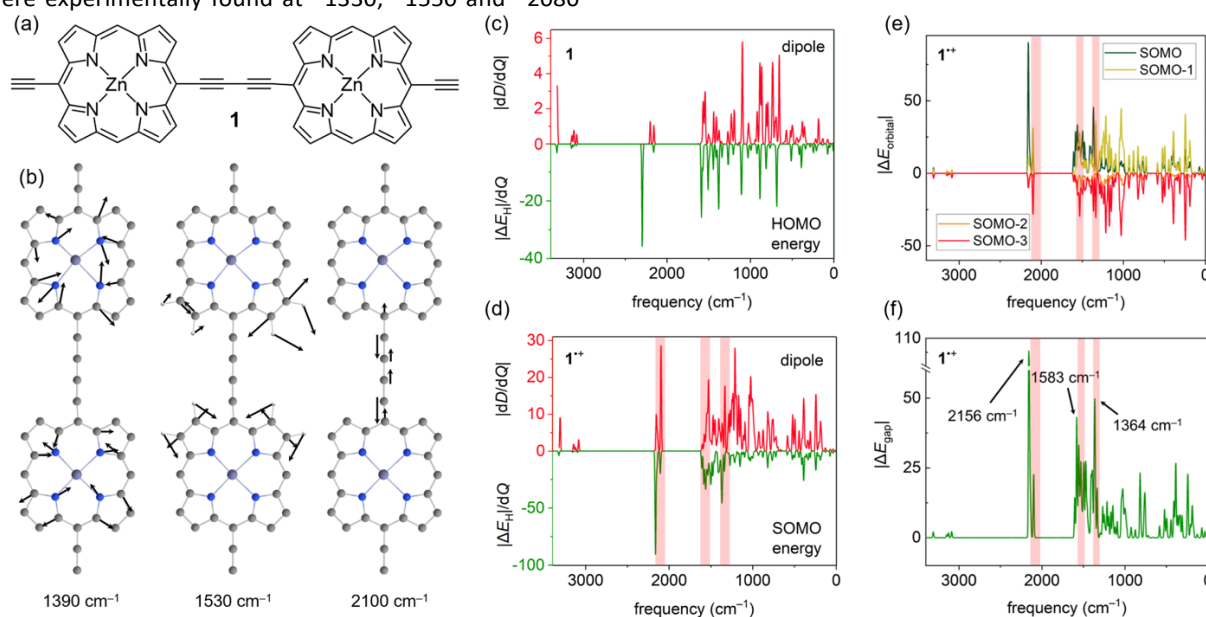
Figure 2. (a) Structure of **1**. (b) Calculated IRAVs of $\mathbf{1}^{\bullet+}$. (c–d) Coupling between the computed IR intensities (positive *y* axis) and derivatives of frontier orbital energies (negative *y* axis) in (c) **1** and (d) $\mathbf{1}^{\bullet+}$. Note the different *y* scales. (e) Contribution of lower-lying orbitals of $\mathbf{1}^{\bullet+}$. (f) Modulation of the fundamental gap ΔE_{gap}/dQ_i in $\mathbf{1}^{\bullet+}$ with molecular vibrations.

An advantage of using ΔE_{gap} instead of the computed IR spectrum is that modes with no IR intensity ($dD/dQ_i = 0$) due to symmetry can also be IRAVs; indeed, some of the first IRAVs were observed in Raman-active modes.[24] In case of $\mathbf{1}^{\bullet+}$, the symmetric stretch of the butadiyne linker at 2156 cm^{-1} (see Figure 1f and S2) is IR forbidden, but it is strongly coupled to the ground electronic state as it decreases the conjugation between the two porphyrins.

In conclusion, we have presented a simple approach for investigating the influence of individual modes on molecular properties, based on calculating orbital energy derivatives with respect to molecular vibrations. By applying this approach to the Thiel's benchmark set of small organic molecules, we demonstrated that it can in most cases correctly identify the vibrations that are most strongly coupled to the vertical excitation energies by using only a ground-state calculation, which is significantly more efficient than using many excited-state calculations.

Molecules with unusually strong coupling between electronic and vibrational states show intense infrared active bands. Using a porphyrin dimer radical cation as an example, we showed how infrared spectrum can be decomposed into orbital contributions, finding a strong coupling between the IRAVs and the singly occupied molecular orbital (SOMO), but also a significant effect of orbitals up to SOMO–3. Finally, we showed that the sensitivity of frontier orbital energies to nuclear movement can be used to identify IRAVs.

Code for calculating orbital derivatives with respect to normal modes and building characteristic geometries at some temperature using eq 4 is provided at https://github.com/lisa-schroeder/mode-resolved-molecular-properties.

Conflicts of interest

There are no conflicts to declare.

Acknowledgements

References

1. R. E. Blankenship, D. M. Tiede, J. Barber, G. W. Brudvig, G. Fleming, M. Ghirardi, M. R. Gunner, W. Junge, D. M. Kramer, A. Melis, T. A. Moore, C. C. Moser, D. G. Nocera, A. J. Nozik, D. R. Ort, W. W. Parson, R. C. Prince and R. T. Sayre, *Science*, 2011, **332**, 805-809.
2. C. C. Page, C. C. Moser, X. Chen and P. L. Dutton, *Nature*, 1999, **402**, 47-52.
3. S. Ho Choi, B. Kim and C. D. Frisbie, *Science*, 2008, **320**, 1482-1486.
4. M. Schreiber, M. R. Silva-Junior, S. P. A. Sauer and W. Thiel, *J. Chem. Phys.*, 2008, **128**.
5. P.-F. Loos, D. A. Matthews, F. Lipparini and D. Jacquemin, *J. Chem. Phys.*, 2021, **154**.
6. A. Kubas, F. Gajdos, A. Heck, H. Oberhofer, M. Elstner and J. Blumberger, *Phys. Chem. Chem. Phys.*, 2015, **17**, 14342-14354.
7. D. Manna, J. Blumberger, J. M. L. Martin and L. Kronik, *Mol. Phys.*, 2018, **116**, 2497-2505.
8. D. Toffoli, M. Quarin, G. Fronzoni and M. Stener, *J. Phys. Chem. A*, 2022, **126**, 7137-7146.
9. J. O. Thomas, B. Limburg, J. K. Sowa, K. Willick, J. Baugh, G. A. D. Briggs, E. M. Gauger, H. L. Anderson and J. A. Mol, *Nat. Commun.*, 2019, **10**, 4628.
10. S. Bai, R. Mansour, L. Stojanović, J. M. Toldo and M. Barbatti, *J. Mol. Model.*, 2020, **26**, 107.
11. T. J. H. Hele, B. Monserrat and A. M. Alvertis, *J. Chem. Phys.*, 2021, **154**, 244109.
12. K. Lambropoulos, A. M. Alvertis, A. Morphis and C. Simserides, *Phys. Chem. Chem. Phys.*, 2022, **24**, 7779-7787.
13. D. Huang, H. Yao, Y. Cui, Y. Zou, F. Zhang, C. Wang, H. Shen, W. Jin, J. Zhu, Y. Diao, W. Xu, C.-a. Di and D. Zhu, *J. Am. Chem. Soc.*, 2017, **139**, 13013-13023.
14. J. Sukegawa, C. Schubert, X. Zhu, H. Tsuji, D. M. Guldi and E. Nakamura, *Nat. Chem.*, 2014, **6**, 899-905.
15. L. Matasović, B. Panić, M. Bubaš, H. Vančik, I. Biljan and I. Rončević, *J. Mater. Chem. C*, 2022, **10**, 5433-5446.
16. E. J. Baerends, O. V. Gritsenko and R. van Meer, *Phys. Chem. Chem. Phys.*, 2013, **15**, 16408-16425.
17. M. Bürkle, J. K. Viljas, T. J. Hellmuth, E. Scheer, F. Weigend, G. Schön and F. Pauly, *Phys. Status Solidi B*, 2013, **250**, 2468-2480.
18. A. D. Becke, *J. Chem. Phys.*, 1993, **98**, 5648-5652.
19. P. K. Nayak, *Synthetic Metals*, 2013, **174**, 42-45.
20. W. J. Kendrick, M. Jirásek, M. D. Peeks, G. M. Greetham, I. V. Sazanovich, P. M. Donaldson, M. Towrie, A. W. Parker and H. L. Anderson, *Chem. Sci.*, 2020, **11**, 2112-2120.
21. D. P. Arnold, R. D. Hartnell, G. A. Heath, L. Newby and R. D. Webster, *ChemComm*, 2002, DOI: 10.1039/B200803N, 754-755.
22. M. D. Peeks, C. E. Tait, P. Neuhaus, G. M. Fischer, M. Hoffmann, R. Haver, A. Cnossen, J. R. Harmer, C. R. Timmel and H. L. Anderson, *J. Am. Chem. Soc.*, 2017, **139**, 10461-10471.
23. C. A. Jiménez-Hoyos, B. G. Janesko and G. E. Scuseria, *Phys. Chem. Chem. Phys.*, 2008, **10**, 6621-6629.24. R. Österbacka, C. P. An, X. M. Jiang and Z. V. Vardeny, *Science*, 2000, **287**, 839-842.